# Erosion-induced isostatic rebound triggers extension in low convergent mountain ranges

P. Vernant[1], F. Hivert[1], J. Chéry[1], P. Steer[2], R. Cattin[1], and A. Rigo[3]
[1]Géosciences Montpellier, CNRS-Université Montpellier 2, Montpellier 34095, France
[2]Géosciences Rennes, Université de Rennes 1, Rennes 35095 , France
[3]Institut de Recherche en Astrophysique et Planétologie, Observatoire Midi-Pyrénées, Toulouse 31400, France

## ABSTRACT

Mechanisms that control seismic activity in low strain rate areas such as western Europe remain poorly understood. For example, in spite of low shortening rates of <0.5 mm/yr, the Western Alps and the Pyrenees are underlain by moderate but frequent seismicity detectable by instruments. Beneath the elevated part of these mountain ranges, analysis of earthquake focal mechanisms indicates extension, which is commonly interpreted as the result of gravitational collapse. Here we show that erosional processes are the predominant control on present-day deformation and seismicity. We demonstrate, using finite element modeling, that erosion induces extension and rock uplift of the elevated region of mountain ranges accommodating relatively low overall convergence. Our results suggest that an erosion rate of ~1 mm/yr can lead to extension in mountain ranges accommodating significant shortening of <3 mm/yr. Based on this study, the seismotectonic framework and seismic hazard assessment for low strain rate areas need to be revisited, because erosion-related earthquakes could increase seismic hazard.

## INTRODUCTION

Strain rates across western Europe are so low that they have not yet been fully quantified (Nocquet, 2012). Contrary to the Eastern Alps, which undergo significant shortening, the upper bound on horizontal motion across the Pyrenees and the Western Alps is ~0 ± 0.5 mm/yr, indicating that these two ranges can be considered to be part of the stable Western Eurasian plate in terms of horizontal motion. However, both ranges have moderate but frequent instrumentally detected seismicity. Available focal mechanisms show normal faulting in regions of moderate to high elevations, with an extension direction normal to the main ridge axis of these mountain ranges, and compression in the Western Alpine foreland (Delacou et al., 2004; Chevrot et al., 2011).

This extensional strain pattern, associated with minor or no horizontal motion, has been interpreted as due to gravitational collapse, which is defined as a gravity-driven flow of orogenic crust under its own weight (England, 1982; Dewey, 1988; Ménard and Molnar, 1988; Rey et al., 2001; Champagnac et al., 2006; Selverstone, 2005; Molnar, 2009). Therefore, gravitational potential energy in a thickened crust is released via lateral spreading, inducing thinning of the lithosphere, extension within the range, and shortening and thickening of the foreland (Dewey, 1988).

If gravitational collapse is the main process occurring in the Pyrenees and in the Western Alps, the vertical rock motion observed by GPS should be downward (Avouac and Burov, 1996). No data have been yet reported for the Pyrenees, but the most elevated region of the Swiss Alps displays GPS- and leveling-derived uplift rates that can reach 2 mm/yr (Brockmann et al., 2012). These geodetic rates are consistent with geomorphic observations (Champagnac et al., 2007) suggesting an erosion rate of 0.5 mm/yr. Champagnac et al. (2007) proposed that the erosion of the Western Alps could explain a part of the modern vertical motions through isostatic rebound. Previous studies have shown that there is a tradeoff between gravitational collapse, erosion, and mountain growth (Avouac and Burov, 1996). However, little attention has been paid to the impact of erosion on present-day deformation in mountain ranges accommodating low convergence rates (Jadamec et al., 2007).

## NUMERICAL MODEL OF EROSION-INDUCED DEFORMATION

We use a two-dimensional finite element model (ADELI 2D; http://www.isteem.univ-montp2.fr/PERSO/chery/adeli_web/index.htm) to test if erosional surface processes and isostatic balance can explain extension below the highest topography of mountain ranges with low convergence rate. We do not aim at specifically reproducing the present-day deformation in western European ranges, but discuss our results in the light of these mountain ranges. The model accounts for the elasto-visco-plastic rheology of the lithosphere (see the GSA Data Repository[1] for details). The erosion rate of the topographic surface is taken proportional to the slope (Beaumont et al., 2001; Steer et al., 2011), and the induced isostatic response is enforced by a uniform hydrostatic pressure condition at the base of the model. Both the modeled initial geometry (i.e., a 200-km-wide and 3-km-high triangular topography compensated by a crustal root; Fig. 1) and geotherm are taken to be representative of the Western Alps and Pyrenees (Lucazeau and Vasseur, 1989).

We first run the model from 0 to 1 m.y. without convergence (i.e., horizontal boundary conditions are set to 0 mm/yr) or erosion. Small horizontal displacements of ~20 m distributed over ~150 km occur in the first 0.2 m.y. This motion is related to the incomplete force balance within the mountain range due to lateral density gradients. Strain rate rapidly vanishes after 0.2 m.y. once equilibrium is reached, showing that no gravitational collapse takes place permanently. The gravitational force is counterbalanced by the strength of the upper crust that
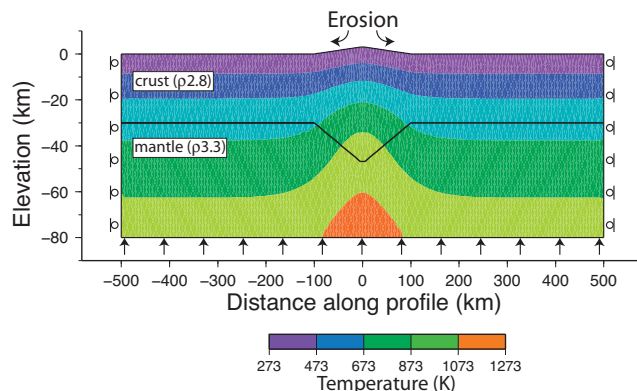


Figure 1. Model initial geometry and setup. Base of model is submitted to hydrostatic forces; vertical displacement of edges is free, while its horizontal component is imposed to 0 mm/yr from 0 to 1 m.y. and then to convergence rate (0–3 mm/yr) from 1 to 2 m.y. Note vertical exaggeration compared to horizontal axis. ρ is the rock density in g/cm³.
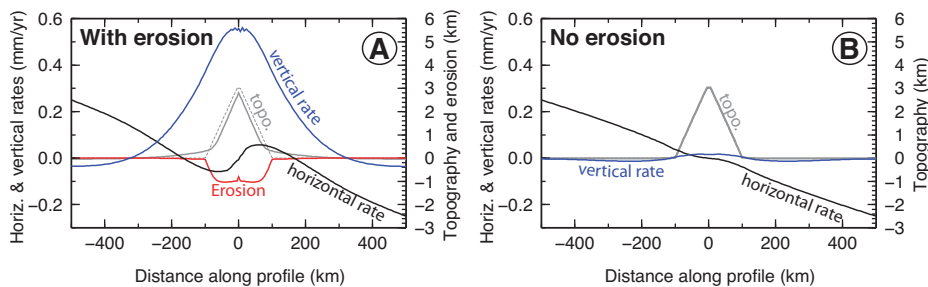
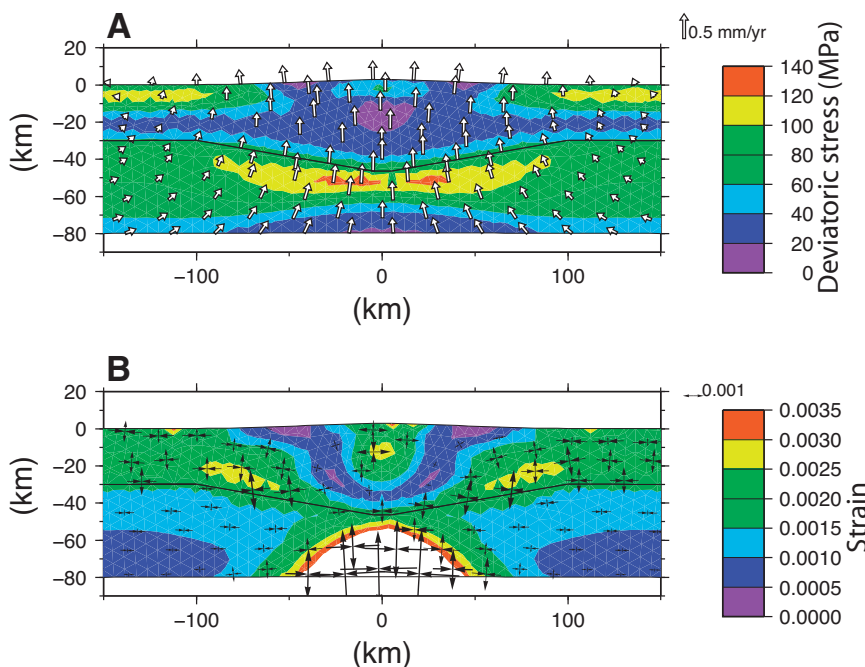may reach several megapascals, according to the frictional parameters used.

Then, between 1 and 2 m.y., we impose 0.5 mm/yr of overall shortening and an average erosion rate of 0.75 mm/yr. For this period of time, we compute the horizontal and vertical velocities of the surface elements (Fig. 2A). As soon as the erosion and compression start at 1 m.y., uplift due to isostatic unbalanced is initiated and is coeval with extension in the mountain core. The erosion induces as much as 0.55 mm/yr of uplift broadly distributed over the topography and 0.2 mm/yr of extension (Fig. 2A) in the inner part of the range. As a consequence, shortening in the foreland is enhanced and reaches 0.7 mm/yr rather than the expected value of 0.5 mm/yr (overall convergence). If erosion is set to 0 from 1 to 2 m.y., no extension occurs in the inner range, and vertical velocity rates are marginal, showing that the upper crust can withstand the gravitational force (Fig. 2B).

At the final time step (2 m.y.), the motion induced by the isostatic rebound and overall shortening results in high deviatoric stresses in the plastic upper crust and uppermost mantle (Fig. 3A). Low deviatoric stress zones are not only restricted to the low-viscosity lower crust and the mantle, but also occur apart from the high topography between compressional and extensional regimes in the upper crust. The velocity field depicts the motion associated with isostatic rebound, with upward motion of both the mantle and crust beneath the range. This uplift associated with the horizontal velocities produces convergent motion in the mantle (compression) and divergent motio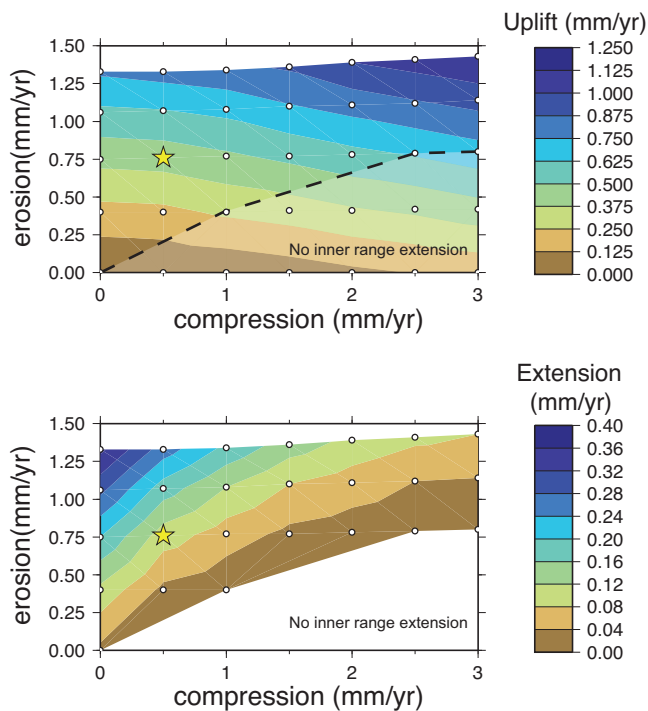n in the crust (extension). This is better illustrated by the strain tensors (Fig. 3B), which reveal that extension may extend down to a depth of 20 km, in agreement with the depth of the seismicity in western Europe (Delacou et al., 2004; Chevrot et al., 2011).

To test the sensitivity of our results with respect to the erosion law we use, we also ran experiments for uniform erosion and diffusion laws (see the Data Repository for details). We found that the onset of uplift and extension is mostly sensitive to the average erosion rate and is only weakly affected by the chosen law. We also ran 35 experiments to study the effects of erosion versus the overall convergence rate (Fig. 4). Average erosion rates range from 0 to 1.4 mm/yr and convergence rates range from 0 to 3 mm/yr. For a mountain range within a stable plate interior (i.e., without overall convergence), extension occurs for any erosion rate. It is interesting that low erosion is more efficient than moderate compression to induce rock uplift, implying that extension beneath the highest part of the mountain is still possible if the average erosion rate is high enough. For example, even with 3 mm/yr of overall convergence, the crust will still undergo extension if the average erosion rate is higher than 0.8 mm/yr. The results (see Fig. 4) suggest that extension could occur even with higher convergence rates.

A key feature of the mechanism involved here to trigger extension is the efficiency of the isostatic response. For the chosen rheological law and a geotherm typical of western European lithosphere, the uplift rate is ~75% of erosion rate. In mountains embedded in a colder lithosphere, the amplitude of the isostatic response becomes a small fraction of the erosion rate. In such a case, extension in the inner range is not likely to occur.

## DISCUSSION AND GEODYNAMIC IMPLICATIONS

These results shed new light on the strain mechanism at work in mountain belts undergoing erosion and moderate convergence rates on their boundaries. First, our simple model accounts for the extension observed in low convergence mountain ranges. The extensional strain regime in the inner part of the model is consistent with the normal faulting focal mechanisms that extend through the upper crust of the Western Alps and the Pyrenees (Delacou et al., 2004; Chevrot et al., 2011). It has also been shown that intense erosion occurred during the late Quaternary and Holocene in the central and Occidental Alps, with an average denudation rate of 0.6–0.7 mm/yr (Champagnac et al., 2009). Given that the GPS-determined uplift rate is ~2 mm/yr in the high range, erosion-induced rock uplift can only explain a part of the vertical motions. If a steady-state process and local isostatic rebound are considered, the mean rock uplift rate should be less than the



Figure 2. Erosion and velocity rates of mountain range surface. Horizontal (black line) and vertical (blue line) velocity rates were obtained at steady state (after 2 m.y.). A: For reference model with average erosion rate of 0.75 mm/yr. B: For model with no erosion. Both models are submitted to 0.5 mm/yr of convergence. Initial (gray dotted line) and final topography (topo., gray line) are plotted, as well as cumulated erosion (red line).



Figure 3. Erosion-induced stress and strain rate in mountain range. Results are shown for reference model (erosion rate of 0.75 mm/yr and convergence rate of 0.5 mm/yr) after 2 m.y. (steady state). A: Velocity field and deviatoric stresses. B: Strain and strain tensor.

**Figure 4. Erosion, compression, and erosion-induced rock uplift for surface measurements. Top: Rock uplift as function of average erosion and convergence rates. Bottom: Horizontal extension in range as function of average erosion and convergence rates. Yellow star indicates reference model presented in Figures 2A and 3.**

associated with horizontal extension both in the upper and lower crust. More important, in the first case the range is undergoing uplift, while in the latter case it is subsiding. It is interesting that we found no clear evidence of gravitational collapse for the western Europe mountain ranges, and instead we propound that their uplift and seismic deformation are in agreement with the erosion-induced extension model.
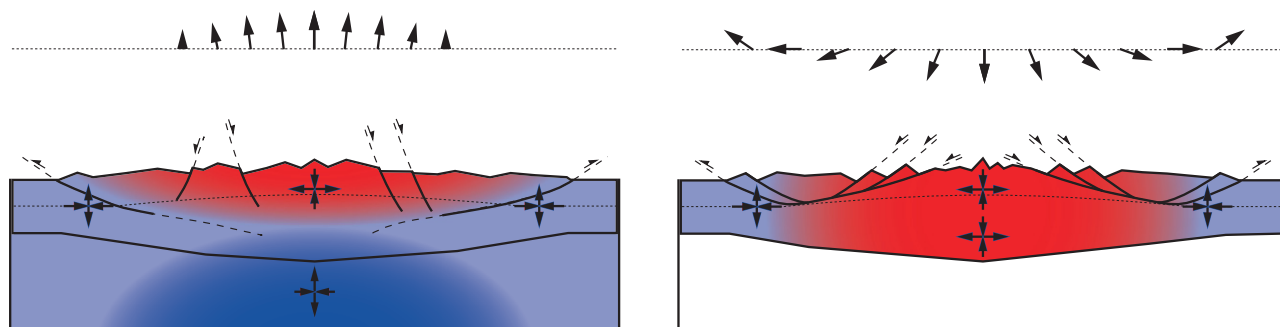
## CONCLUSIONS

Our simple two-dimensional model suggests a causal relationship between erosion, uplift, and extension in the core of weakly active mountains belts. As pointed out previously (Thatcher et al., 1999; Champagnac et al., 2007), gravitational collapse of the topography is not likely to be the only process responsible for the internal deformation of the mountain ranges and elevated plateaus. Our results are at odds with the generally accepted tectonic paradigm that tectonic activity occurs primarily in response to horizontal motions. In the case of European lithosphere, where geodetic vertical motions associated with time-variable loads such as erosion, sedimentation, and glaciations dominate the horizontal signal, this paradigm may not hold. A reevaluation of the seismotectonic framework and associated seismic hazard in low convergent mountain ranges is therefore necessary in light of this new source of fault loading.

### REFERENCES CITED

Avouac, J.P., and Burov, E.B., 1996, Erosion as a driving mechanism of intracontinental mountain growth: Journal of Geophysical Research, v. 101, p. 17747–17769, doi:10.1029/96JB01344.

Barletta, V.R., Ferrari, C., Diolaiuti, G., Carnielli, T., Sabadini, R., and Smiraglia, C., 2006, Gla-

average erosion. However, glacial isostatic rebound models suggest as much as 0.9 mm/yr of uplift in the western Alps due to the glacier shrinkage after the Little Ice Age (Barletta et al., 2006) and as much as 0.3 mm/yr of uplift due to the Last Glacial Maximum (Stocchi et al., 2005). Therefore, the geodetic vertical velocities could be the sum of these three processes. Although we did not account for ice unloading in our model, one can conjecture that glacial isostatic response induces a similar extensional stress state in the upper crust below the highest elevated region. The high uplift rates of the central Western Alps could also be partly induced by overthickened crust with respect to its isostatic depth (Kissling, 2008).

It is easy and straightforward to understand the mechanisms at play when a mountain range embedded in a plate with no horizontal deformation is eroded. The isostatic uplift induced by erosion creates a flexure, which in turn creates low horizontal extension. This mechanism has been previously used to explain a reduction of normal stresses in the upper crust sufficient to unclamp preexisting faults close to failure equilibrium (Calais et al., 2010). Having extension within a range that is submitted to convergence is less trivial; however, as for the case without convergence, if the uplift related to erosion is higher than the one induced by shortening, extension occurs. From a tectonic point of view, gravitational collapse or erosion-induced extension are very difficult to distinguish using only geological observations (Fig. 5); however, differences exist. The erosion-induced uplift is associated with horizontal shortening in the upper mantle and lower crust, and extension in the upper crust, whereas gravitational collapse is



**Figure 5. Erosion-induced extension versus gravitational collapse. Expected surface displacements (arrows above cross sections) and strain tensors for range submitted to erosion (left) and for gravitational collapse of a range (right) are shown. Dotted line indicates brittle-ductile transition. Main difference between erosion and gravitational collapse–induced deformation is vertical motion of surface and location of extension. Moreover, and in contrast to gravitational collapse, in erosion-induced extension, lower crust is submitted to horizontal compression.**

cier shrinkage and modeled uplift of the Alps: Geophysical Research Letters, v. 33, L14307, doi:10.1029/2006GL026490.

Beaumont, C., Jamieson, R.A., Nguyen, M.H., and Lee, B., 2001, Himalayan tectonics explained by extrusion of a low-viscosity crustal channel coupled to focused surface denudation: Nature, v. 414, p. 738–742, doi:10.1038/414738a.

Brockmann, E., Ineichen, D., Marti, U., Schaer, S., and Schlatter, A., 2012, Determination of tectonic movements in the Swiss Alps using GNSS and leveling, *in* Kenyon, S., et al., eds., Geodesy for planet Earth: International Association of Geodesy Symposia, v. 136, p. 689–695.

Calais, E., Freed, A.M., Van Arsdale, R., and Stein, S., 2010, Triggering of New Madrid seismicity by late Pleistocene erosion: Nature, v. 466, p. 608–611, doi:10.1038/nature09258.

Champagnac, J.D., Sue, C., Delacou, B., Tricart, P., Allanic, C., and Burkhard, M., 2006, Miocene lateral extrusion in the inner western Alps revealed by dynamic fault analysis: Tectonics, v. 25, TC3014, doi:10.1029/2004TC001779.

Champagnac, J.D., Molnar, P., Anderson, R.S., Sue, C., and Delacou, B., 2007, Quaternary erosion-induced isostatic rebound in the western Alps: Geology, v. 35, p. 195–198, doi:10.1130 /G23053A.1.

Champagnac, J.D., Schlunegger, F., Norton, K., von Blanckenburg, F., Abbuhl, L.M., and Schwab, M., 2009, Erosion-driven uplift of the modern Central Alps: Tectonophysics, v. 474, p. 236–249, doi:10.1016/j.tecto.2009.02.024.

Chevrot, S., Sylvander, M., and Delouis, B., 2011, A preliminary catalog of moment tensors for the Pyrenees: Tectonophysics, v. 510, p. 239–251, doi:10.1016/j.tecto.2011.07.011.

Delacou, B., Sue, C., Champagnac, J.D., and Burkhard, M., 2004, Present-day geodynamics in the bend of the western and central Alps as constrained by earthquake analysis: Geophysical Journal International, v. 158, p. 753–774, doi:10.1111/j.1365-246X.2004.02320.x.

Dewey, J.F., 1988, Extensional collapse of orogens: Tectonics, v. 7, p. 1123–1139, doi:10.1029 /TC007i006p01123.

England, P.C., 1982, Some numerical investigations of large scale continental deformation, *in* Hsü, K.J., ed., Mountain building processes: New York, Academic Press, p. 129–139.

Jadamec, M.A., Turcotte, D., and Howell, P., 2007, Analytic models for orogenic collapse: Tectonophysics, v. 435, p. 1–12, doi:10.1016/j .tecto.2007.01.007.

Kissling, E., 2008, Deep structure and tectonics of the Valais—And the rest of the Alps: Bulletin fuer Angewandte Geologie, v. 13, no. 2, p. 3–10.

Lucazeau, F., and Vasseur, G., 1989, Heat flow density data from France and surrounding margins: Tectonophysics, v. 164, p. 251–258, doi:10.1016 /0040-1951(89)90018-8.

Ménard, G., and Molnar, P., 1988, Collapse of Hercynian Tibetan Plateau into a late Paleozoic European basin and range province: Nature, v. 334, p. 235–237, doi:10.1038/334235a0.

Molnar, P., 2009, The state of interactions among tectonics, erosion, and climate: A polemic: GSA Today, v. 19, no. 7, p. 44–45, doi:10.1130 /GSATG00GW.1.

Nocquet, J.-M., 2012, Present-day kinematics of the Mediterranean: A comprehensive overview of GPS results: Tectonophysics, doi:10.1016/j .tecto.2012.03.037.

Rey, P., Vanderhaeghe, O., and Teyssier, C., 2001, Gravitational collapse of the continental crust: Definition, regimes and modes: Tectonophysics, v. 342, p. 435–449, doi:10.1016/S0040 -1951(01)00174-3.

Selverstone, J., 2005, Are the Alps collapsing?: Annual Review of Earth and Planetary Sciences, v. 33, p. 113–132, doi:10.1146/annurev .earth.33.092203.122535.

Steer, P., Cattin, R., Lavé, J., and Godard, V., 2011, Surface Lagrangian remeshing: A new tool for studying long-term evolution of continental lithosphere from a 2D numerical modeling: Computers & Geosciences, v. 27, p. 1067–1074.

Stocchi, P., Spada, G., and Cianetti, S., 2005, Isostatic rebound following the Alpine deglaciation: Impact on the sea level variations and vertical movements in the Mediterranean region: Geophysical Journal International, v. 162, p. 137–147, doi:10.1111/j.1365-246X.2005.02653.x.

Thatcher, W., Foulger, G.R., Julian, B.R., Svarc, J.L., Quilty, E., and Bawden, G.W., 1999, Present-day deformation across the Basin and Range province, western United States: Science, v. 283, p. 1714–1718, doi:10.1126/science.283.5408.1714.